Cite this: DOI: 10.1039/c0xx00000x

www.rsc.org/xxxxxx

ARTICLE TYPE

A soluble bispentacenequinone precursor for creation of directly 6,6′-linked bispentacenes and a tetracyanobipentacenequinodimethane

Kazuki Tanaka,[a] Naoki Aratani,[a,b] Daiki Kuzuhara,[a] Sadaaki Sakamoto,[c] Tetsuo Okujima,[c] Noboru Ono,[c] Hidemitsu Uno[c] and Hiroko Yamada*[,a,d]

Received (in XXX, XXX) Xth XXXXXXXXX 20XX, Accepted Xth XXXXXXXXX 20XX

DOI: 10.1039/b000000x

We have synthesized 13,13'-(3,5-bis(trifluoromethyl)phenyl)-6,6'-bipentacene from a soluble bispentacenequinone precursor. Bispentacene takes orthogonal conformation in the solid state and exhibits four reversible redox potentials. In addition, a tetracyanobipentacenequinodimethane was obtained for the first time from the pure bispentacenequinone.

Introduction

Organic molecular materials have attracted great interest in recent years as a potential low-cost alternative to amorphous silicon-based semiconductors for many applications in electronics.[1] Among these, the electronic properties of pentacene are exceptionally well investigated, making it a common benchmark in the field of organic electronic devices.[2] The pentacene oligomers, however, remain virtually unexplored, mainly because of their chemical instability and low solubility. Hitherto only two examples of pentacene dimers were so far reported.[3,4]

A potential precursor of bispentacene is bispentacenequinone **2** (Scheme 1). Surprisingly, however, **2** has been “unavailable” even its simple structure, since the conventional synthetic route for **2** is via oxidation of pentacenone **1**, which results in the formation of an inseparable mixture of **2** and pentacenequinone **3** due to their low solubility.[3,5] Thus, soluble precursors with thermally or photochemically removable leaving groups have intrinsically merited.[6-10] Recently we have reported the photochemical conversion in solutions or in films of an α-diketone precursor into the corresponding acene with the release of two CO molecules.[6,11] Beside them, thermal reaction has also been applied to the synthesis of larger acenes by taking advantage of the unique features of bicyclo[2.2.2]octadiene (BCOD).[12] Such a thermal method has enabled us to prepare benzoporphyrinoids which can be used as materials for the solar cell and the organic field effect transistor (OFET) devices.[13]

Now we describe the synthesis of directly 6,6′-linked bispentacene via the retro-Diels–Alder reaction of BCOD-bispentacene precursors (Scheme 2). Our work on soluble oligoacene precursors has shown that, in addition to providing increased solubility and chemical stability, the crystalline nature becomes remarkable. We here also report the application of our precursor method to the synthesis and characterization of an extended tetracyanoquinodimethane (TCNQ) derivative, tetracyanobipentacenequinodimethane (TBPQ, **11**).

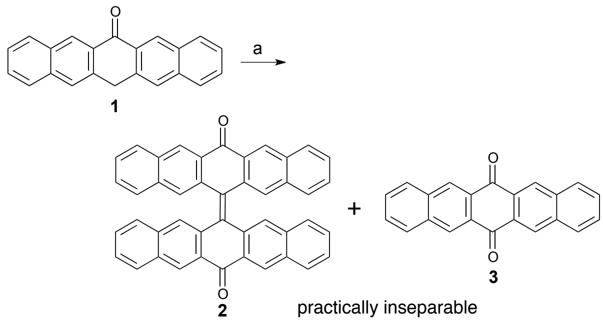

Scheme 1. Conventional synthesis of bispentacenequinone **2**. a) Pyridine-*N*-oxide, piperidine, $FeSO_4$, pyridine.

Results and discussion

Synthesis of directly 6,6'-linked bispentacene

The route for the synthesis of BCOD-bispentacenequinone precursor **7** starts from a Diels–Alder reaction of *p*-benzoquinone with 5,6-dimethylene-bicyclo[2.2.2]oct-2-ene (**4**) to form the bisadduct, then subsequent dehydrogenation provided the bicycloanthraquinone **5** (Scheme 2).[14] The quinone **5** was reduced with lithium aluminium hydride (LAH) and the anthrone **6** obtained was oxidized by the Matur's conditions to get bianthrone **7** in 77% yield.[15] As expected, **7** is soluble in common organic solvents (>5 mg/ml in $CHCl_3$) so that it would be a versatile reagent for many reactions (vide infra).

The structure of **7** was confirmed by its ^{1}H-NMR and high-resolution electrospray ionization time-of-flight (HR-ESI-TOF) mass spectroscopies (Supporting Information). Slow vapour diffusion of methanol into a chloroform solution of **7** gave its good crystals suitable for X-ray diffraction analysis (Figure 1).‡ The crystal structure of **7** revealed a butterfly-shaped skeleton unambiguously, in which the anthracene core is distorted into a saddle conformation.

At first, we tried to prepare an authentic bispentacene from **7** as a non-substituted mother skeleton. After several optimization experiments, we found that the stepwise reduction of **7** with LAH and then DIBAL gave **8a** in 31% yield. The structure of **8a** was revealed by a single-crystal X-ray diffraction analysis (Figure 1c).‡ In the crystal, the two pentacene units in **8a** display a perpendicular conformation of about 88°. Then we performed the retro-Diels–Alder reaction of **8a**. The thermogravimetric (TG) analysis of **8a** is shown in Figure S15. The weight loss of **8a** started at around 250°C and stopped after 300°C. Although the weight loss of **8a** was 15% that corresponds to the elimination of four ethylene molecules, its ^{1}H-NMR, ESI-TOF mass, and UV-vis absorption spectroscopies indicated that a lot of undesired compounds were produced after the formation of **9a**, suggesting the chemical instability of **9a** (Figures S16 and S17). Next, with 13,13'-free bispentacene precursor **8a** in hand, we thus examined its halogenation for metal-catalyzed cross-coupling reactions. Though the bromination of **8a** proceeded with NBS in THF to provide **8b**, unfortunately the yield was as low as 19% (Figure 1d).‡ It is noteworthy that **8b** can be a potential unit for making graphene nano-ribbons.[16]

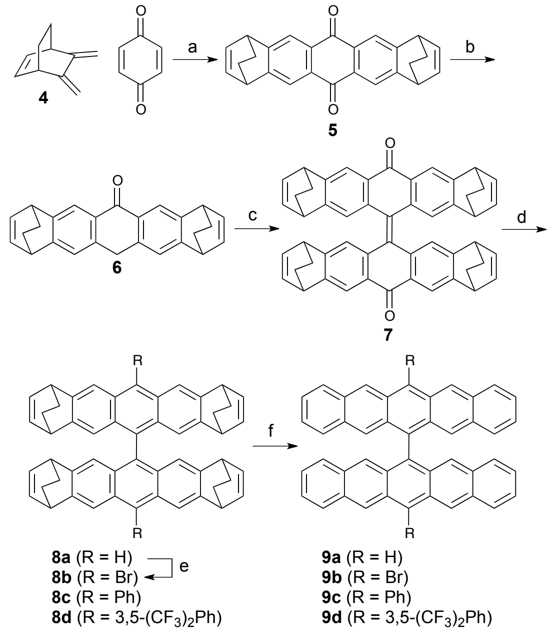

Scheme 2. Synthesis of bispentacenes **9a-d**. Reaction conditions: a) i) $CHCl_3$ ii) KOH/EtOH, 60% (2 steps). b) Lithium aluminium hydride (LAH), then 6 N HCl, THF, 66%. c) Pyridine-*N*-oxide, piperidine, $FeSO_4$, pyridine, 80%. d) LAH, then 6 N HCl, DIBAL 31% (2 steps) for **8a**, ArLi then NaH_2PO_2, NaI for **8c** (67%) and **8d** (28%), e) NBS, 19%, f) heating, 93% for **9d**.

As has been extensively demonstrated in the pentacene chemistry, its stability should depend on the substituents on the periphery.[17] So we next tried to synthesize the 13,13'-bis-arylated bispentacenes. Treatment of **7** with phenyllithium, subsequent deoxygenation and aromatization with sodium iodide and sodium hypophosphite,[18] gave the bispentacene precursor **8c** in 46% yields (Figure 1e).‡ The retro-Diels–Alder reaction of **8c** afforded almost pure **9c** judging from its TG analysis, ^{1}H-NMR, HR-ESI-TOF mass, and UV-vis absorption spectroscopies (Figures S19-22), while it was difficult to remove a small amount of byproducts. Finally, a good electron withdrawing substituent, 3,5-bis(trifluoromethyl)phenyl group was introduced. **8d** was prepared by the same method to **8c** (Figure 1f).‡ **8d** smoothly underwent thermal conversion at 300°C for 10 min, and after the measurement of TG, the pure, stable, and soluble **9d** was obtained at last without any problems like a zoo of byproducts for **9a-c**. We assume that the electron withdrawing groups make the molecule tougher against oxidative ambient conditions owing to the stabilized HOMO level. The structure of **9d** is fully consistent with the spectroscopic data. HR-ESI-TOF mass spectrum detected the parent ion peak at m/z = 978.371 (calcd for $C_{58}H_{40}N_4$ = 978.216 $[M]^+$) (Figure S13). The ^{1}H NMR spectrum of **9d** in CD_2Cl_2 exhibits aromatic protons at 8.32, 7.85, 7.77, 7.30, 7.21, and 7.07 ppm. The structure of **9d** was unambiguously determined by single crystal X-ray diffraction analysis (Figures 1g and 1h).‡ Pentacene planes are highly planar and exhibit a small tilting dihedral angle from orthogonal conformation (78°). Importantly, in the crystal, a pair of slipped π-π stacking of both pentacene planes in **9d** results in the formation of two-dimensional grid-like network structure along *a*-*b* plane of crystal lattice (Figure 2). This is a new potential structural motif for pentacene based semi-conducting materials.[3]

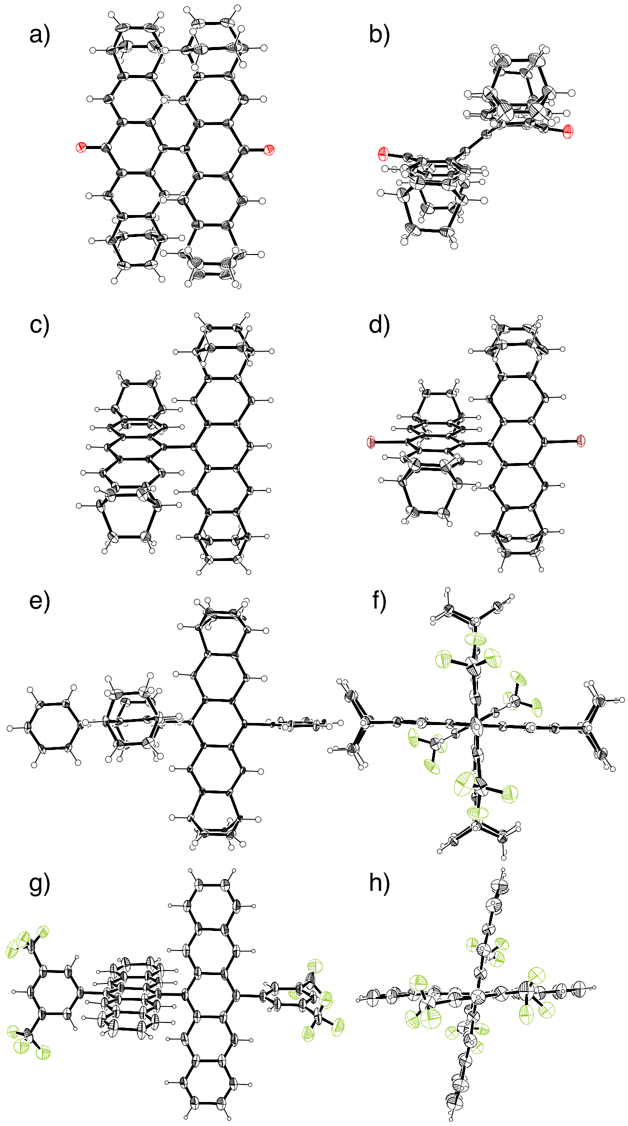

Figure 1. X-ray crystal structures of a) **7** (top view), b) **7** (side view), c) **8a**, d) **8b**, e) **8c**, f) **8d**, g) **9d** (top view) and h) **9d** (side view). Solvent molecules and disordered parts are omitted for clarity.

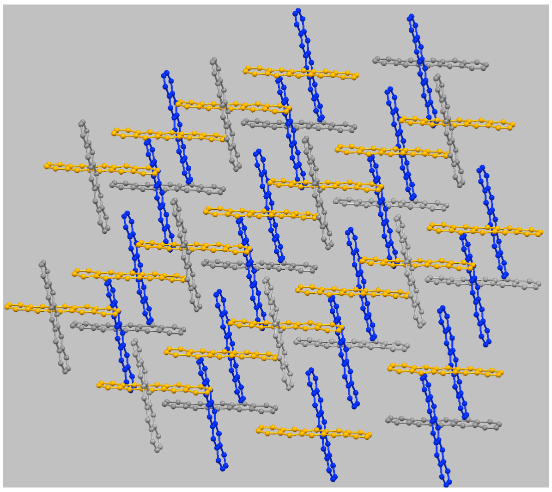

Figure 2. Crystal lattice view of **9d** from *a-b* plane. For clarity, pentacene units are shown as a ball-and-stick model, and hydrogen atoms and 3,5-bis(trifluoremethyl)phenyl groups are omitted.

UV-vis absorption spectra of **8d** and **9d** along with pentacene are shown in Figure 3. Compared to pentacene (λ_{max} = 578 nm in $CHCl_3$), **9d** exhibits distinctly red-shifted absorption at 612 nm (ε = 2.0 × 10^4 $M^{-1}cm^{-1}$; optical HOMO–LUMO gap is 2.02 eV) with the vibrational bands and a small stokes shift (159 cm^{-1}), indicating a considerable electronic communication between two pentacene units with rigid skeleton in **9d**. This is also confirmed by cyclic voltammetry (CV). The CV of **9d** in CH_2Cl_2 displays four redox potentials at –1.79, –1.72, 0.32, and 0.46 V (vs ferrocene/ferrocenium$^+$ ion couple) as fully reversible waves (Figure 4). These split one-electron oxidations and reductions for each pentacene unit in bispentacene should arise from the influence of the charge of first-generated pentacene radical ion. The electrochemical HOMO–LUMO gap is thus 2.04 eV.

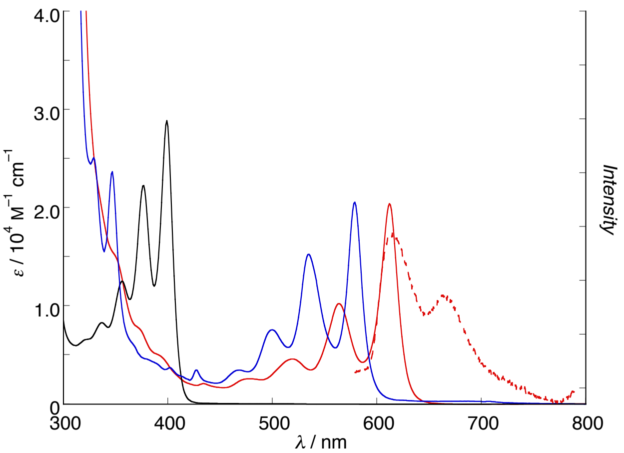

Figure 3. UV-vis absorption spectra of pentacene (blue), **8d** (black), and **9d** (red) and fluorescence spectrum of **9d** (dashed red) in $CHCl_3$. Absorption of pentacene is normalized at the absorption maximum of **9d** (612 nm).

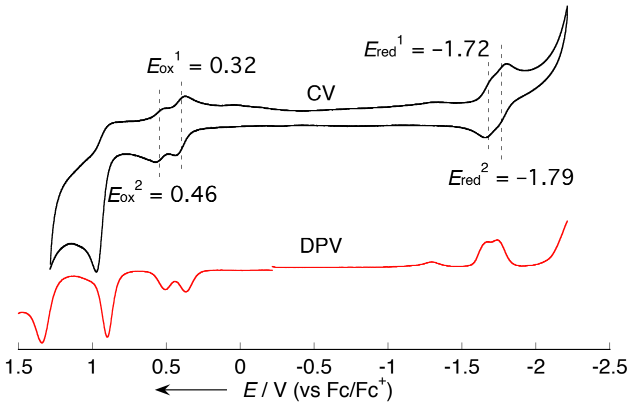

Figure 4. Cyclic voltammogram (black) and differential pulse voltammogram (red) of **9d** in CH_2Cl_2.

Synthesis of tetracyanobipentacenequinodimethane (TBPQ)

The successful creation of bispentacene **9d** from bispentacene-quinone **7** made us aware that the soluble precursor **7** could be available for synthesis of other "insoluble" products. Thus, we tried to synthesize an extended TCNQ analogue, tetracyano-bipentacenequinodimethane (TBPQ) **11** (Scheme 3). In recent years, much efforts have been made to develop new electron acceptor molecules whose structures would enhance the electrical conductivities in their molecular electronic devices.[19] Among these, TCNQ has been widely used as an acceptor molecule to form highly conducting charge transfer complexes. The simple extension of the π-system of TCNQ has been shown to lead to a regulation of the intra- and intermolecular Coulomb repulsion in their dianion forms. However, one often confronts a dilemma that an electron-deficient π-expanded molecule has low solubility in common organic solvents, which hampers the isolation and the characterization of the desired compounds.

Taking advantage of the soluble character of **7**, first we tested a condensation reaction of **7** with malononitrile (Scheme 3). The reaction in the presence of $TiCl_4$ as catalyst was successful in pyridine and toluene at high temperature, affording **10** in 10% yield. As expected, **10** is soluble in various solvent and the structure was confirmed by its ^{1}H-NMR and HR-ESI-TOF mass spectroscopies, and single crystal X-ray diffraction analysis.[‡] The crystal structure of **10** revealed a butterfly-shaped skeleton unambiguously, in which the dicyanomethylene groups are deviated from the anthracene mean plane due to the steric hindrance by the hydrogen atoms at the peri-positions (Figure 5). The planes NC-C-CN and the central benzene ring make an angle of 35.0°. The deviation between two mean planes of the central benzene ring is 1.40 Å. Unfortunately, however, the thermal reaction of **10** afforded unidentified products so that we changed the synthetic route.

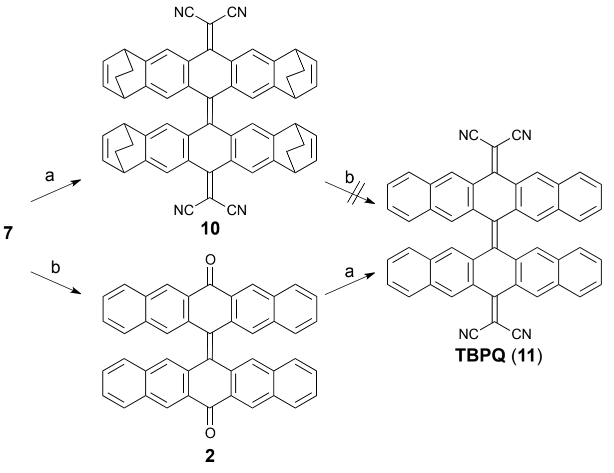

Scheme 3. Synthesis of TBPQ **11**. Reaction conditions: a) malononitrile, $TiCl_4$ (2.2% for **10**, 10% for **11**) b) heating, 98%.

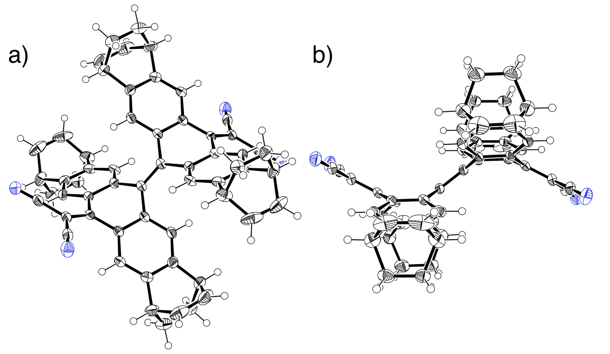

Figure 5. X-ray crystal structure of **10**; a) perspective view and b) side view. Solvent molecules and disordered parts are omitted for clarity.

From TG analysis of **7**, we observed the retro-Diels–Alder reaction started at around 200°C and ended at around 250°C (Figure S25). The characterization of a pyrolytic compound obtained quantitatively was successfully done, the structure of which is shown in Figure 5.‡ Interestingly, the quinone **2** exhibits polymorphism (Figure 6 and Figure S37). The side views of these crystal structures clearly indicate the flexibility of bispentacenequinone framework. This is the first practical isolation of bispentacenequinone **2**.

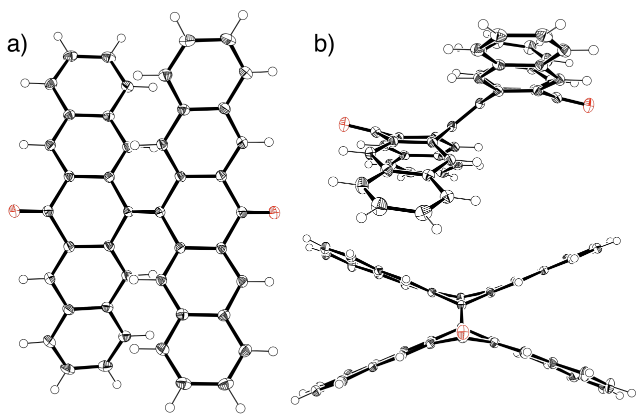

Figure 6. X-ray crystal structure of **2**; a) perspective view and b) side view. Solvent molecules and disordered parts are omitted for clarity.

With the pure **2** in hand, a condensation reaction of **2** was performed with malononitrile, affording **11** in 10% yield. Although the solubility of **11** is limited, the structure of **11** is fully consistent with the spectroscopic data. HR-ESI-TOF mass spectrum detected the parent ion peak of **11** at *m/z* = 680.201 (calcd for $C_{58}H_{40}N_4$ = 680.200 $[M]^-$) (Figure S14). The ^{1}H NMR spectrum of **11** in CD_2Cl_2 exhibits aromatic protons at 8.71, 8.01, 7.77, 7.54, and 7.41 ppm.

The CV measurements of the new compound **11** along with **10** and tetracyanopentacenequinodimethane have been carried out in THF at room temperature. TBPQ **11** exhibits one reversible single-wave reduction at –1.51 V, implying the electron storage ability of **11** (Figure S28). Deep negative shift of the reduction potential of **11** compared to that of tetracyanopentacenequinodimethane (–1.06 V, Figure S28) indicates that the elongation of the distance between dicyanomethylene units by pentacene makes its electron accepting ability moderate.

Conclusions

In summary, we have synthesized 13,13'-(3,5-bis(trifluoromethyl)phenyl)-6,6'-bipentacene **9d** from the soluble bispentacenequinone precursor **7**. **9d** takes orthogonal conformation and 2D grid-like network in the solid state, and exhibits four reversible redox potentials. In addition, TBPQ **11** was obtained for the first time from the pure bispentacenequinone **2**. A series of TCNQs have received much electrochemical attention; however, there was insufficient data to actually measure it. Its instability, combined with poor solubility, has made its preparation and study difficult. Soluble precursor method leads us to believe that this strategy enables the preparation of higher acenes with the improved stability and solubility. Complexation study of TBPQ with various donors is now under way.

Acknowledgements

This work was partly supported by Grants-in-Aid for Scientific Research (No. 22350083) and for Young Scientists (A) (No. 23685030), the Green Photonics Project in NAIST supported by MEXT, and CSTP initiated FIRST program (No. 22350083) by JSPS. We thank Mr. S. Katao, NAIST, for the X-ray diffraction analysis and Ms. Y. Nishiyama, Ms. Y. Nishikawa, and Ms. M. Yamamura, NAIST, for the mass spectroscopy measurements.

Notes and references

[a] *Graduate School of Materials Science, Nara Institute of Science and Technology (NAIST), Takayama-cho, Ikoma, Nara 630-0192 Japan. Fax: +81-743-72-6042; Tel: +81-743-72-6030; E-mail:aratani@ms.naist.jp, hyamada@ms.naist.jp*

[b] *PRESTO, Japan Science and Technology Agency (JST).*

[c] *Department of Chemistry and Biology, Graduate School of Science and Engineering, Ehime University, Bunkyo–cho 2–5, Matsuyama, 790–8577 Japan.*

[d] *CREST, Japan Science and Technology Agency (JST).*

† Electronic Supplementary Information (ESI) available: Experimental details of the synthesis and spectroscopic analytical data of new compounds. For ESI and crystallographic data in CIF or other electronic format. See DOI: 10.1039/b000000x/

‡ Crystallographic data for **7**: $C_{52}H_{40}O_2$, *Mw* = 696.89, monoclinic, space group $P2_1/n$ (No. 14), a = 10.2853(4), b = 12.1795(4), c = 14.7576(5) Å, β = 106.4150(10)°, V = 1773.34(10) Å^3, ρ_{calcd} = 1.305 g/cm^3, Z = 2, R_1 = 0.0668 [I > 2.0$\sigma(I)$], Rw = 0.1868 (all data), GOF = 1.060.

Crystallographic data for **8a**: $C_{52}H_{42}$·$(C_4H_{10}O)$, *Mw* = 740.98, triclinic, space group *P*-1 (No. 2), a = 11.1984(5), b = 11.3073(5), c = 16.8154(7) Å, α = 73.8090(10), β = 86.8410(10), γ = 75.5040(10)°, V = 1979.44(15) Å^3, ρ_{calcd} = 1.243 g/cm^3, Z = 2, R_1 = 0.0697 [$I > 2.0\sigma(I)$], *Rw* = 0.2343 (all data), GOF = 1.055. Crystallographic data for **8b**: $C_{52}H_{40}Br_2$·0.58$(CHCl_3)$·0.75(CH_3OH), *Mw* = 914.38, monoclinic, space group *C*2/*c* (No. 15), a = 41.930(4), b = 15.3835(14), c = 18.8623(18) Å, β = 102.9120(10)°, V = 11859.0(19) Å^3, ρ_{calcd} = 1.536 g/cm^3, Z = 12, R_1 = 0.0994 [$I > 2.0\sigma(I)$], *Rw* = 0.3153 (all data), GOF = 1.040. Crystallographic data for **8c**: $C_{64}H_{50}$·3$(CHCl_3)$, *Mw* = 1177.14, monoclinic, space group $P2_1/c$ (No. 14), a = 24.018(3), b = 10.2100(14), c = 22.028(3) Å, β = 90.352(2)°, V = 5401.5(13) Å^3, ρ_{calcd} = 1.448 g/cm^3, Z = 4, R_1 = 0.0774 [$I > 2.0\sigma(I)$], *Rw* = 0.2429 (all data), GOF = 1.015. Crystallographic data for **8d**: $C_{68}H_{46}F_{12}$·4$(CHCl_3)$, *Mw* = 1568.52, monoclinic, space group *C*2/*c* (No. 15), a = 24.6901(5), b = 21.1291(5), c = 17.5492(4) Å, β = 130.4530(10)°, V = 6966.4(3) Å^3, ρ_{calcd} = 1.496 g/cm^3, Z = 4, R_1 = 0.0693 [$I > 2.0\sigma(I)$], *Rw* = 0.2151 (all data), GOF = 1.064. Crystallographic data for **9d**: $C_{60}H_{30}F_{12}$, *Mw* = 978.84, monoclinic, space group *C*2/*c* (No. 15), a = 13.271(10), b = 30.35(2), c = 12.823(10) Å, β = 121.152(11)°, V = 4420(6) Å^3, ρ_{calcd} = 1.471 g/cm^3, Z = 4, R_1 = 0.1051 [$I > 2.0\sigma(I)$], *Rw* = 0.3304 (all data), GOF = 1.035. Crystallographic data for **10**: $C_{58}H_{40}N_4$·2$(CHCl_3)$, *Mw* = 1031.68, monoclinic, space group *C*2/*c* (No. 15), a = 17.4912(6), b = 12.3477(4), c = 23.7674(8) Å, β = 93.3020(10)°, V = 5124.7(3) Å^3, ρ_{calcd} = 1.337 g/cm^3, Z = 4, R_1 = 0.0685 [$I > 2.0\sigma(I)$], *Rw* = 0.1949 (all data), GOF = 1.059. Crystallographic data for **2**: $C_{44}H_{24}O_2$·$(CHCl_3)$, *Mw* = 704.00, monoclinic, space group *C*2/*c* (No. 15), a = 24.8385(6), b = 11.3087(2), c = 12.6953(3) Å, β = 112.6680(10)°, V = 3290.54(13) Å^3, ρ_{calcd} = 1.421 g/cm^3, Z = 4, R_1 = 0.0584 [$I > 2.0\sigma(I)$], *Rw* = 0.1529 (all data), GOF = 1.070. CCDC-923852 (**7**), 923855 (**8a**), 923856 (**8b**), 923853 (**8c**), 923854 (**8d**), 923857 (**9d**), 923849 (**10**), and 923850 (**2**) contain the supplementary crystallographic data for this paper. These data can be obtained free of charge from The Cambridge Crystallographic Data Centre via www.ccdc.cam.ac.uk/data_request/cif.

1 A. R. Murphy and J. M. J. Fréchet, *Chem. Rev*. 2007, **107**, 1066–1096.

2 (a) R. Ruiz, D. Choudhary, B. Nickel, T. Toccoli, K.-C. Chang, A. C. Mayer, P. Clancy, J. M. Blakely, R. L. Headrick, S. Iannotta and G. G. Malliaras, *Chem. Mater*. 2004, **16**, 4497–4508; (b) L. Gross, F. Mohn, N. Moll, P. Liljeroth and G. Meyer, *Science*, 2009, **325**, 1110–1114.

3 X. Zhang, X. Jiang, J. Luo, C. Chi, H. Chen and J. Wu, *Chem. Eur. J.* 2010, **16,** 464–468.

4 S. Li, Z. Jia, K. Nakajima, K.-i. Kanno and T. Takahashi, *J. Org. Chem*. 2011, **76**, 9983−9987.

5 S. Xiao, S. J. Kang, Y. Wu, S. Ahn, J. B. Kim, Y.-L. Loo, T. Siegrist, M. L. Steigerwald, H. Li and C. Nuckolls, *Chem. Sci*., 2013,**4**, 2018–2023.

6 (a) H. Uno, Y. Yamashita, M. Kikuchi, H. Watanabe, H. Yamada, T. Okujima, T. Ogawa and N. Ono, *Tetrahedron Lett*. 2005, **46**, 1981–1983; (b) H. Yamada, Y. Yamashita, M. Kikuchi, H. Watanabe, T. Okujima, H. Uno, T. Ogawa, K. Ohara and N. Ono, *Chem. Eur. J*. 2005, **11**, 6212–6220; (c) Y. Zhao, R. Mondal and D. C. Neckers, *J. Org. Chem*. 2008, **73**, 5506–5513; (d) S. Katsuta, H. Yamada, T. Okujima and H. Uno, *Tetrahedron Lett*. 2010, **51**, 1397–1400.

7 (a) A. R. Brown, A. Pomp, D. M. de Leeuw, D. B. M. Klaassen, E. E. Havinga, P. Herwig and K. Müllen, *J. Appl. Phys*. 1996, **79**, 2136–2138; (b) P. T. Herwig and K. Müllen, *Adv. Mater*. 1999, **11**, 480–483.

8 (a) A. Afzali, C. D. Dimitrakopoulos and T. L. Breen, *J. Am. Chem. Soc*. 2002, **124**, 8812–8813; (b) A. Afzali, C. D. Dimitrakopoulos and T. O. Graham, *Adv. Mater*. 2003, **15**, 2066–2069; (c) K. P. Weidkamp, A. Afzali, R. M. Tromp and R. J. Hamers, *J. Am. Chem. Soc*. 2004, **126**, 12740–12741; (d) A. Afzali, C. R. Kagan and G. P. Traub, *Synth. Met*. 2005, **155**, 490–494; (e) D. Zander, N. Hoffmann, K. Lmimouni, S. Lenfant, C. Petit and D. Vuillaume, *Microelectron. Eng*. 2005, **80**, 394–397; (f) T. Akinaga, S. Yasutake, S. Sasaki, O. Sakata, H. Otsuka and A. Takahara, *Chem. Lett*. 2006, **35**, 1162–1163.

9 (a) K.-Y. Chen, H.-H. Hsieh, C.-C. Wu, J.-J. Hwang and T. J. Chow, *Chem. Commun*. 2007, 1065–1067; (b) T.-H. Chuang, H.-H. Hsieh, C.-K. Chen, C.-C. Wu, C.-C. Lin, P.-T. Chou, T.-H. Chao and T. J. Chow, *Org. Lett*. 2008, **10**, 2869–2872.

10 J. Strating, B. Zwanenburg, A. Wagenaar and A. C. Udding, *Tetrahedron Lett*. 1969, **10**, 125–128.

11 (a) R. Mondal, B. K. Shah and D. C. Neckers, *J. Am. Chem. Soc*. 2006, **128**, 9612–9613; (b) R. Mondal, R. M. Adhikari, B. K. Shah and D. C. Neckers, *Org. Lett*. 2007, **9**, 2505–2508; (c) R. Mondal, C. Tönshoff, D. Khon, D. C. Neckers and H. F. Bettinger, *J. Am. Chem. Soc*. 2009, **131**, 14281–14289; (d) C. Tönshoff and H. F. Bettinger, *Angew. Chem. Int. Ed*. 2010, **49**, 4125–4128.

12 (a) N. Ono, H. Yamada and T. Okujima in *Handbook of Porphyrin Science*, Vol. 2 (Eds.: K. M. Kadish, K. M. Smith and R. Guilard), World Scientific, Singapore, 2010, pp. 1–102, and references cited therein; (b) S. Ito, T. Murashima, N. Ono and H. Uno, *Chem. Commun*. 1998, 1661–1662; (c) D. Kuzuhara, H. Yamada, K. Yano, T. Okujima, S. Mori and H. Uno, *Chem. Eur. J*. 2011, **17**, 3376–3383.

13 (a) M. D. Perez, C. Borek, P. I. Djurovich, E. I. Mayo, R. R. Lunt, S. R. Forrest and M. E. Thompson, *Adv. Mater*. 2009, **21**, 1517–1520; (b) Y. Matsuo, Y. Sato, T. Niinomi, I. Soga, H. Tanaka and E. Nakamura, *J. Am. Chem. Soc*. 2009, **131**, 16048–16050.

14 T. Akiyama, A. Hirao, T. Okujima, H. Yamada, H. Uno and N. Ono, *Heterocycles*, 2007, **74**, 835–842.

15 Y. Mazur, H. Bock and D. Lavie, Can. Pat. Appl. 202993, 1991.

16 J. Cai, P. Ruffieux, R. Jaafar, M. Bieri, T. Braun, S. Blankenburg, M. Muoth, A. P. Seitsonen, M. Saleh, X. Feng, K. Müllen and R. Fasel, *Nature* 2010, **466**, 470–473.

17 (a) K. Ono, H. Totani, T. Hiei, A. Yoshino, K. Saito, K. Eguchi, M. Tomura, J.-i. Nishida and Y. Yamashita, *Tetrahedron*, 2007, **63**, 9699–9704; (b) Y.-M. Wang, N.-Y. Fu, S.-H. Chan, H.-K. Lee and H. N. C. Wong, *Tetrahedron*, 2007, **63**, 8586–8597.

18 W. Cui, Y. Wu, H. Tian, Y. Geng and F. Wang, *Chem. Commun*. 2008, 1017–1019.

19 (a) Y. Fujisaki, M. Mamada, D. Kumaki, S. Tokito and Y. Yamashita, *Jpn. J. Appl. Phys*. 2009, **48**, 111504; (b) Y. Sakamoto, T. Suzuki, M. Kobayashi, Y. Gao, Y. Fukai, Y. Inoue, F. Sato and S. Tokito, *J. Am. Chem. Soc*. 2004, **126**, 8138–8140; (c) M. Mamada, D. Kumaki, J.-i. Nishida, S. Tokito and Y. Yamashita, *ACS Appl. Mater. Interfaces*, 2010, **2**, 1303–1307; (d) B. Yoo, B. A. Jones, D. Basu, D. Fine, T. Jung, S. Mohapatra, A. Facchetti, K. Dimmler, M. R. Wasielewski, T. J. Marks and A. Dodabalapur, *Adv. Mater*. 2007, **19**, 4028–4032. (e) K. Walzer, B. Maennig, M. Pfeiffer, and K. Leo, *Chem. Rev*. 2007, **107**, 1233–1271.